THE JOURNAL OF BIOLOGICAL CHEMISTRY VOL. 286, NO. 7, pp. 5392–5403, February 18, 2011

Negative Regulation of the Endocytic Adaptor Disabled-2 (Dab2) in Mitosis*[S]

Received for publication, July 7, 2010, and in revised form, November 18, 2010 Published, JBC Papers in Press, November 19, 2010, DOI 10.1074/jbc.M110.161851

David Chetrit[‡], Lior Barzilay[‡], Galit Horn[‡§], Tom Bielik[‡§], Nechama I. Smorodinsky[‡§], and Marcelo Ehrlich[‡1]

From the [‡]Department of Cell Research and Immunology, [§]The Alec and Myra Marmot Hybridoma Unit, George S. Wise Faculty of Life Sciences, Tel Aviv University, Tel Aviv 69978, Israel

Mitotic cells undergo extensive changes in shape and size through the altered regulation and function of their membrane trafficking machinery. Disabled 2 (Dab2), a multidomain cargo-specific endocytic adaptor and a mediator of signal transduction, is a potential integrator of trafficking and signaling. Dab2 binds effectors of signaling and trafficking that localize to different intracellular compartments. Thus, differential localization is a putative regulatory mechanism of Dab2 function. Furthermore, Dab2 is phosphorylated in mitosis and is thus regulated in the cell cycle. However, a detailed description of the intracellular localization of Dab2 in the different phases of mitosis and an understanding of the functional consequences of its phosphorylation are lacking. Here, we show that Dab2 is progressively displaced from the membrane in mitosis. This phenomenon is paralleled by a loss of co-localization with clathrin. Both phenomena culminate in metaphase/anaphase and undergo partial recovery in cytokinesis. Treatment with 2-methoxyestradiol, which arrests cells at the spindle assembly checkpoint, induces the same effects observed in metaphase cells. Moreover, 2-methoxyestradiol also induced Dab2 phosphorylation and reduced Dab2/clathrin interactions, endocytic vesicle motility, clathrin exchange dynamics, and the internalization of a receptor endowed with an NP*X*Y endocytic signal. Serine/threonine to alanine mutations, of residues localized to the central region of Dab2, attenuated its phosphorylation, reduced its membrane displacement, and maintained its endocytic abilities in mitosis. We propose that the negative regulation of Dab2 is part of an accommodation of the cell to the altered physicochemical conditions prevalent in mitosis, aimed at allowing endocytic activity throughout the cell cycle.

Disabled-2 (Dab2) is a multidomain mitotic phosphoprotein that functions as a signal modulator and tumor suppressor (1–11) and as a cargo-specific adaptor of clathrin-mediated endocytosis (12–21). Different Dab2 isoforms localize to distinct intracellular compartments. Thus, at steady state, the long isoform (denominated p96 or p82 in different species) localizes to the plasma membrane (14, 18, 20), whereas the short isoform (denominated p67 or p59), which is devoid of a central exon (22), presents a diffuse distribution pattern with a considerable localization to the cell nucleus (2). In accord with its multiple functions, a number of interactors have been identified for Dab2. These include clathrin (14), the adaptor complex 2 (AP2 (20)), NP*X*Y-containing cargo (13–16, 20), and myosin VI (18, 23–25), all related to its endocytic functions, and Dab2-interacting protein (Dab2IP (1)), Src (6), Grb (4), CIN85 (26), axin (7), Smads, and the transforming growth factor β (TGF-β) receptors (9, 10), which enable the signal-modulating potential of Dab2. Dab2 also binds directly to integrins and may thus coordinate changes to cell adhesion, cell motility, membrane trafficking, and signaling (11, 27–30). Taken together, the current picture suggests that the function of Dab2 is regulated by intracellular localization, by association with specific interacting factors, and possibly by post-translational modification. However, the interdependence of these different modes of regulation still remains to be determined and is at the center of this study.

The mitotic shutdown of endocytosis, a mechanism proposed more than 25 years ago (31–33), is a contentious subject (32–36). However, a consensus exists concerning the relocalization of clathrin to the mitotic spindle (37–40), a shutdown of recycling at prophase, and its renewal and functional importance in cytokinesis (34, 41). The notion of a modulation of the functions of endocytic proteins in mitosis is supported by the mitosis-related post-translational modifications of these proteins. Thus, Dab2, epsin, and Eps15 were proposed to undergo a transient cdc2-mediated phosphorylation in mitosis (42, 43). Furthermore, an alteration in the intracellular localization of Dab2 in mitosis has been suggested (14). However, a thorough description of the cell cycle-dependent alterations to the localization and functional interactions of Dab2 and an assessment of the endocytosis of cargo endowed with different internalization signals in mitosis are currently lacking and will be addressed here.

The spindle assembly checkpoint (SAC)[2] is a critical step in the transition from the early to late stages of mitosis (44). Low concentrations of nocodazole, vinblastine, or 2-methoxyestradiol (2ME2) induce an arrest of the cell cycle at the SAC without causing massive microtubule depolymerization (45–47).

* This work was supported in part by Israel Science Foundation Grant 1122/06.

[S] The on-line version of this article (available at http://www.jbc.org) contains supplemental "Experimental Procedures," Figs. 1–6, and Movies 1 and 2.

[1] To whom correspondence should be addressed: Dept. of Cell Research and Immunology, George S. Wise Faculty of Life Sciences, Tel Aviv University, Tel Aviv 69978, Israel. Tel.: 972-3-640-9406; Fax: 972-3-642-2046; E-mail: marceloe@tauex.tau.ac.il.

[2] The abbreviations used are: SAC, spindle assembly checkpoint; CCF, correlation coefficient; LDLR, low density lipoprotein receptor; TβRI, type I TGF-β receptor; VtM, variance to mean ratio; 2ME2, 2-methoxyestradiol; h, human; r, rat.

Cytosol extracts, of cells arrested in this manner, accumulate mitotically phosphorylated endocytic proteins and hamper the invagination of clathrin-coated pits in permeabilized cells (32, 33, 42, 43).

Here, we employ ES-2 ovary cancer cells and 2ME2 to show that the intracellular localization of the p96/p82 isoform of Dab2, its phosphorylation state, and its association with clathrin are cell cycle-dependent. Moreover, in G_2/M-arrested cells, the internalization of endocytic cargo endowed with an NP*XY* signal is inhibited.

EXPERIMENTAL PROCEDURES

Cells—ES-2 cells, human ovarian cancer cells, were a kind gift of Dr. Michal Neeman (Weizmann Institute, Rehovot, Israel). HeLa S3 cells were a kind gift of Dr. Orna Elroy Stein (Tel Aviv University). Cells were grown in DMEM supplemented with 10% fetal calf serum, penicillin/streptomycin, 5 mM glutamine (all from Biological Industries, Beit HaEmek, Israel).

DNA Constructs—pEGFP-CI was from Clontech. The clathrin light chain A fusion construct has been described previously (48). TβRI-158 (a Myc-tagged truncation mutant of the TGF-β type I receptor), TβRI-LDLR (TβRI-158 supplemented with an FDNP*XY* signal), and TβRI-transferring receptor (TβRI-158 supplemented with a Y*XX*Φ signal) have been described previously (49). For the generation of Myc-tagged p82 and p59 constructs and mutants, the Rat p82 cDNA sequence (obtained from Open BioSystems) or Rat p59 (described in Ref. 49) were inserted into the BamHI and NsiI sites of the CMVneoMYC1 vector (a generous gift of Prof. Mia Horowitz, Tel Aviv University). For the list of primers employed in the generation of the various constructs employed in this study see the supplemental "Experimental Procedures".

Drugs and Treatments—2-Methoxyestradiol (Sigma) was kept at 3.3 mg/ml (in ethanol) and employed at 4.4 μM. Roscovitine (Sigma) was kept at 2.8 mg/ml (in DMSO) and employed at 28 μg/ml (80 μM). Nocodazole (Sigma) was kept at 17 mM in DMSO and employed at 50 μM. In control treatments, a similar concentration of vehicle was employed.

Immunochemicals—The following antibodies and reagents were employed in the present study: α-Dab2 (H-110, Santa Cruz Biotechnology); α-α-tubulin (BioLegend); α-clathrin heavy chain (X22, Novus Biologicals); rabbit polyclonal α-phosphothreonine-proline/phosphoserine-proline antibody (ab3944, Abcam); labeled secondary antibodies (Invitrogen); α-epidermal growth factor receptor and α-ERK 1/2 (Cell Signaling); peroxidase-conjugated antibodies (Jackson ImmunoResearch); and biotinylated goat α-rabbit antibody (Amersham Biosciences). ExtrAvidin-peroxidase (E-8386, Sigma). The α-Myc tag hybridoma (9E10) was a generous gift of Prof. Yoav Henis (Tel Aviv University); α-myosin VI was a kind gift from Prof. K. Avraham (Tel Aviv University). To generate mouse monoclonal anti-p96 antibodies, BALB/c 4-week-old female mice were injected subcutaneously with 50 μg of peptide (5′-CESSVQSSPHDSIAIIPPPQSTKPGR-3′; residues 417–442 of p96) cross-linked to keyhole limpet hemocyanin supplemented with Freund's adjuvant and boost-injected with the same formulation 5 and 8 weeks after the original injection. For the generation of hybridomas, hybridization was performed according to Ref. 50.

Cell Lysis for Immunoprecipitation and Immunoblotting—Equal numbers of cells (under the different treatment conditions) were lysed in 150 mM NaCl, 10–20 mM Hepes, pH 7.4, 0.5% Igepal CA-630, 1% Triton, protease, and phosphatase inhibitors (Sigma).

Imaging, Acquisition, Processing, and Quantitation—Cells were imaged with a spinning disk confocal microscope setup (Zeiss 100×, NA 1.4; Yokogawa CSU-22; Zeiss fully automated-inverted 200 M; solid state lasers (473 and 561 nm); piezo controlled Z-stage, temperature controlled chamber) all under the command of Slidebook™. Analysis of co-localization was done in ImageJ using the JACoP plugin (73) to calculate the Van Steensel's CCF with a pixel shift of $\delta = \pm 20$. The maximal Pearson coefficient, obtained in all cases at $\delta x = 0$, was employed in averaging values from different images.

RESULTS

Changes to the Intracellular Localization of Dab2 during the Cell Cycle—The initial objective of this study was to examine the intracellular localization of Dab2 in different stages of the cell cycle. To this end, we fixed, permeabilized, and stained asynchronously growing ES-2 cells (mesenchyme-like human ovarian cancer cells that express considerable amounts of Dab2) against microtubules, DNA, and Dab2; we selected cells according to their DAPI staining pattern and imaged the entire cell volume by confocal microscopy (Fig. 1, *A–F*). For the ensuing analysis, cells were assigned to different stages of the cell cycle according to their microtubule and DNA staining patterns. In Fig. 1, for each cell cycle stage, panels depicting two different planes of representative cells are shown as follows: the plane in contact with the glass, termed bottom plane, which is optimal for the visualization of membrane-bound proteins, and a middle plane of the cell, which is optimal for the visualization of the cytosolic subpopulation of the different proteins in question. In the course of mitosis, Dab2 underwent a marked change in intracellular localization. In interphase cells, Dab2 localized to discrete puncta in both the bottom and top cellular membranes (Fig. 1*A*, the top membrane is visualized in the *middle plane panel* due to the flatness of ES-2 cells in interphase). Contrastingly, as cells progressed through the cell cycle, the fluorescence signal of Dab2 became more diffuse and more prominent in the cell interior (Fig. 1, *B–F*). To quantitatively characterize this alteration in the staining pattern of Dab2, we measured the variance-to-mean (VtM) ratio of the fluorescence signal of Dab2 at the bottom plane of the imaged cells. In accord with its punctate character, in which a few pixels present bright fluorescence on a dark background, the staining of Dab2 in interphase cells presented a high VtM ratio (Fig. 1*G*). Accordingly, the VtM ratio of the Dab2 staining at the bottom plane of cells at all subsequent cell cycle stages was significantly lower (Fig. 1*G*, $p < 0.001$). Taking in account the z-resolution of our imaging conditions (~500 nm) and the diffuse staining pattern obtained in all imaging planes of the mitotic cells, the alteration in the staining pattern of Dab2 is consistent with the loss of

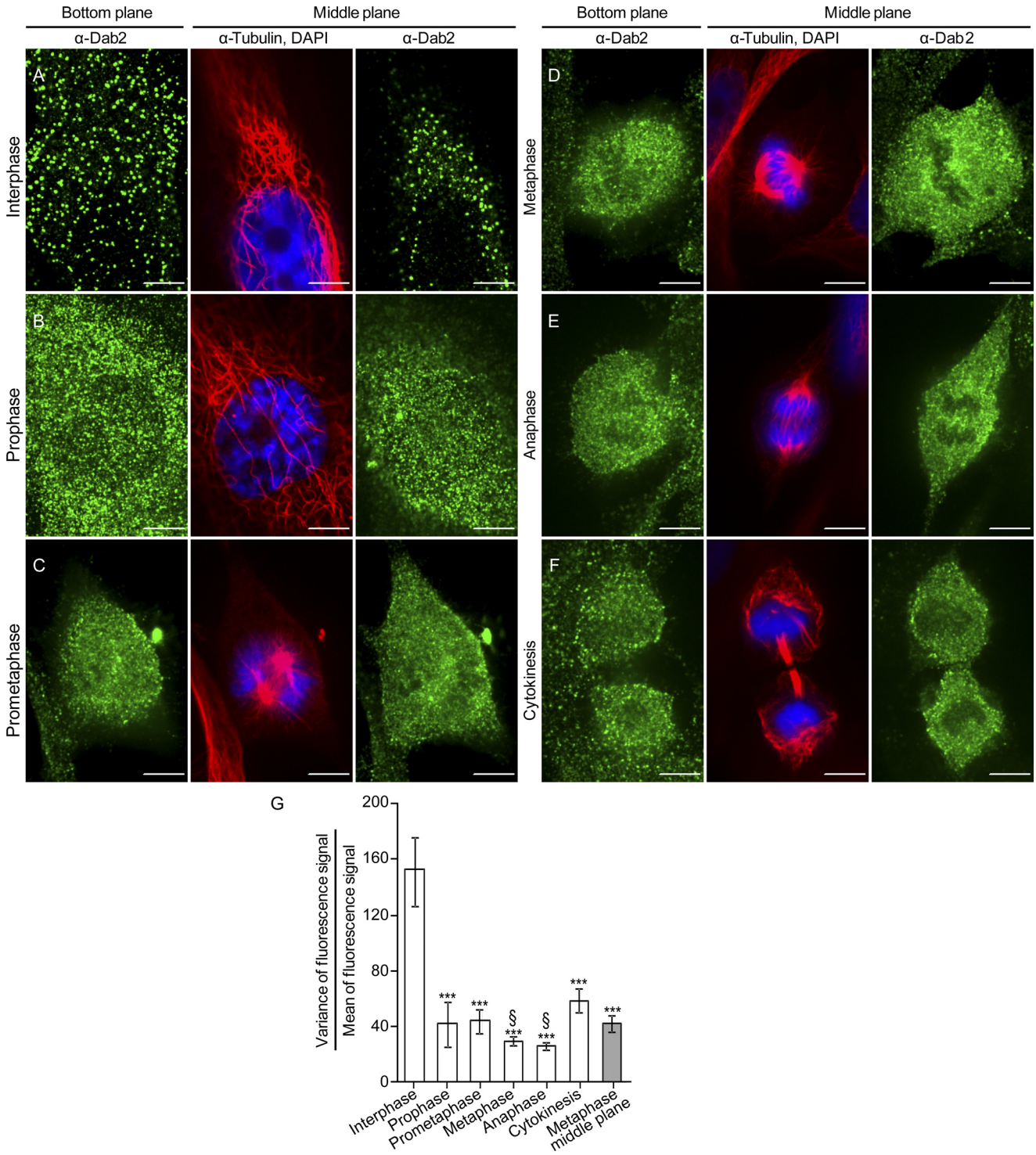

FIGURE 1. **Intracellular staining pattern of Dab2 is altered in mitosis.** *A–F,* unsynchronized ES-2 cells were plated onto glass coverslips. 16 h post-plating, cells were fixed and stained against microtubules, Dab2, and DNA. Cells were imaged by confocal microscopy and assigned different stages of the cell cycle according to the distribution pattern of DNA and microtubules. *Bar,* 10 μm. *G, graph* depicts the quantification of the ratio of the variance-of-fluorescence-signal to the mean of fluorescence-signal (VtM) of Dab2 in the bottom plane of cells imaged as in *A–F*. Values were calculated with Slidebook™. Each *bar* represents the average of 10–17 cells imaged in each condition. Significance was calculated by the Student's *t* test. ***, $p < 0.001$, when comparing the average VtM values obtained in all cell cycle stages to the average VtM of interphase cells; §, $p < 0.001$, when comparing cells in metaphase or anaphase to cells in cytokinesis.

its membrane attachment and of its re-localization to the cytosol. Indeed, the VtM ratio of Dab2 fluorescence in the cytosol (obtained from the middle plane of cells in metaphase) showed a similar value ($p > 0.09$) to the one obtained in the bottom plane of mitotic cells. Interestingly, the VtM ratio of cells in cytokinesis yielded an intermediate value (between the values obtained in interphase and metaphase; $p < 0.001$). To further confirm these observations, an analogous experiment

and analysis were performed with HeLa cells and yielded similar results (supplemental Fig. 1). Taken together, the above presented data reinforce the notion of the cyclical nature of the alterations to the intracellular localization of Dab2.

Next, we performed a similar experiment, staining this time for clathrin heavy chain, Dab2, and DNA. In interphase cells, Dab2 and clathrin showed extensive co-localization in membrane-localized puncta (representative images Fig. 2*A*, and quantification of the maximum Pearson's coefficient, Fig. 2*G*). Moreover, no co-localization was observed among Dab2 and clathrin at the trans-Golgi network (TGN) (Fig. 2*A*, *lower right-hand corner*). In addition to the observed effects on the intracellular distribution of Dab2, progression through mitosis also altered the staining pattern of clathrin, which showed a prominent recruitment to the mitotic spindle (similarly to the effect observed previously (39, 40)). In accord with a relocalization to different intracellular compartments, the correlation of the Dab2 and clathrin fluorescence signals is significantly decreased throughout mitosis (Fig. 2*G*). Moreover, here too the lowest correlation coefficient between Dab2 and clathrin was observed in metaphase cells, and the correlation coefficient observed in cytokinesis presented an intermediate value, both suggestive of the cyclical nature of the processes that dictate Dab2 localization and its co-localization with clathrin.

2ME2 Induces the Phosphorylation of Dab2—Although microscopy allowed for the analysis of Dab2 localization in single unperturbed cells, an enrichment of the population of mitotic cells is necessary for the study of putative post-translational modifications and alterations to Dab2 interactions in mitosis. Perturbation of microtubule dynamics is an effective way of promoting cell cycle arrest in mitosis. Nocodazole, which induces microtubule depolymerization, has been extensively employed as a cell cycle arresting agent in the study of endocytosis (33). Here, to minimize effects stemming from microtubule depolymerization, we opted to employ 2ME2, a promising chemotherapy drug that arrests cells at the SAC without massively depolymerizing microtubules (Fig. 3*B*) (47, 51). Initially, we verified by flow cytometry that the conditions employed (4.4 μM 2ME2, 14–16 h) arrested a considerable proportion of ES-2 cells in G_2/M without leading to apoptosis (detectable by sub-G_1 DNA content and induced by concentrations of 2ME2 $\geq$10 μM; Fig. 3*A*). In a typical experiment, treatment with 2ME2 led to an accumulation of ~40–60% of the cells with an ~4*n* DNA content. In addition, ~20–30% of the cells accumulate in S-phase. To confirm these results, we stained attached cells under different treatment conditions with DAPI. In a typical experiment employing 4.4 μM 2ME2 for 14–16 h, ~30–50% of the cells showed a rounded morphology and condensed DNA (indicative of the G_2/M arrest). In subsequent microscopy-based experiments involving 2ME2 treatment, condensed DNA (in fixed cells) and cellular morphology (in live cells) were employed as criteria for the selection of cells. Next, we assayed the intracellular distribution of Dab2 in 2ME2-arrested cells by immunofluorescence (Fig. 3*B*). Here, similarly to cycling cells in mitosis (Figs. 1 and 2), Dab2 was diffuse throughout the cytoplasm (Fig. 3*B*). Importantly, 2ME2 reduced the VtM of Dab2 fluorescence (a reduction of 83 $\pm$ 1%, $p < 2E-06$) and the co-localization with clathrin (Fig. 3*B* and quantified in supplemental Fig. 3). To further investigate the effects of 2ME2 on the distribution of Dab2 between the cytoplasmic and membrane fractions, we submitted ES-2 cells (treated or not with 2ME2) to cellular fractionation. Similarly to the results obtained by immunofluorescence, 2ME2 induced an increase in the distribution of Dab2 to the cytoplasmic fraction (S100, supplemental Fig. 2*A*; 1.5-fold increase in the typical experiment presented here). Furthermore, upon 2ME2 treatment, the cytoplasmically localized Dab2 migrated with a distinct upward mobility shift (discussed in detail below). In addition, 2ME2 induced a marked decrease in the distribution of Dab2 to the particulate fraction (P100, supplemental Fig. 2*A*). Moreover, a mild detergent extraction of the P100 fraction confirmed that upon treatment with 2ME2, a very small amount of Dab2 remained associated with membranes (supplemental Fig. 2*A*). Immunoblotting of whole-cell lysates confirmed that in cells arrested in G_2/M with 2ME2, Dab2 underwent a marked upward shift in its apparent molecular weight (Fig. 3*C*). The proportion of the p96 isoform of Dab2, which undergoes the upward shift (~40–80%, depending on the experiment), was in direct proportion to the percentage of cells arrested in G_2/M (measured by FACS in parallel to the immunoblotting and from the same pool of treated cells in each experiment). The observed shift is in line with the reported phosphorylation of Dab2 in HeLa cells arrested in G_2/M with nocodazole (43). Accordingly, nocodazole (50 μM, 16 h) also induced a similar shift in p96 in ES-2 cells (Fig. 3*C*). However, the percentage of p96, which underwent the alteration in migration, was consistently higher in cells treated with 2ME2, possibly indicating a more precise arrest at the SAC stemming from the different mechanism of interference with microtubule dynamics. To confirm that the molecular weight shift stemmed from the phosphorylation of Dab2, we immunoprecipitated Dab2 from 2ME2- or vehicle-treated cells and treated a subset of the samples with calf intestinal phosphatase. Indeed, de-phosphorylation by calf intestinal phosphatase completely abolished the shift in molecular weight, confirming phosphorylation as the reason for the shift induced by 2ME2 (Fig. 3*D*). To further characterize the effect of 2ME2 on Dab2 phosphorylation, we repeated the above-described experiments with HeLa cells. Here too, 2ME2 efficiently induced (to a greater extent than nocodazole) the phosphorylation and shift in the apparent molecular weight of Dab2 (data not shown).

He *et al.* (43) proposed that cdc2 phosphorylates Dab2 in mitosis. Their proposition was based on the detection of an interaction between Dab2 and cdc2 in cells, on *in vitro* phosphorylation data, and on the inhibitory effect of roscovitine on the phosphorylation of Dab2. Based on this assessment, we next probed for the effects of roscovitine on Dab2 phosphorylation in ES-2 cells treated with 2ME2. Roscovitine (80 μM, 16 h), when applied in combination with 2ME2 (4.4 μM, 16 h), inhibited the phosphorylation of Dab2 (see the lack of upward molecular weight shift in supplemental Fig. 3*D*) and preserved its punctate membrane distribution and its co-localization with clathrin (supplemental Fig. 3, *A* and *B*). However, roscovitine also inhibited the cell cycle arrest induced by 2ME2

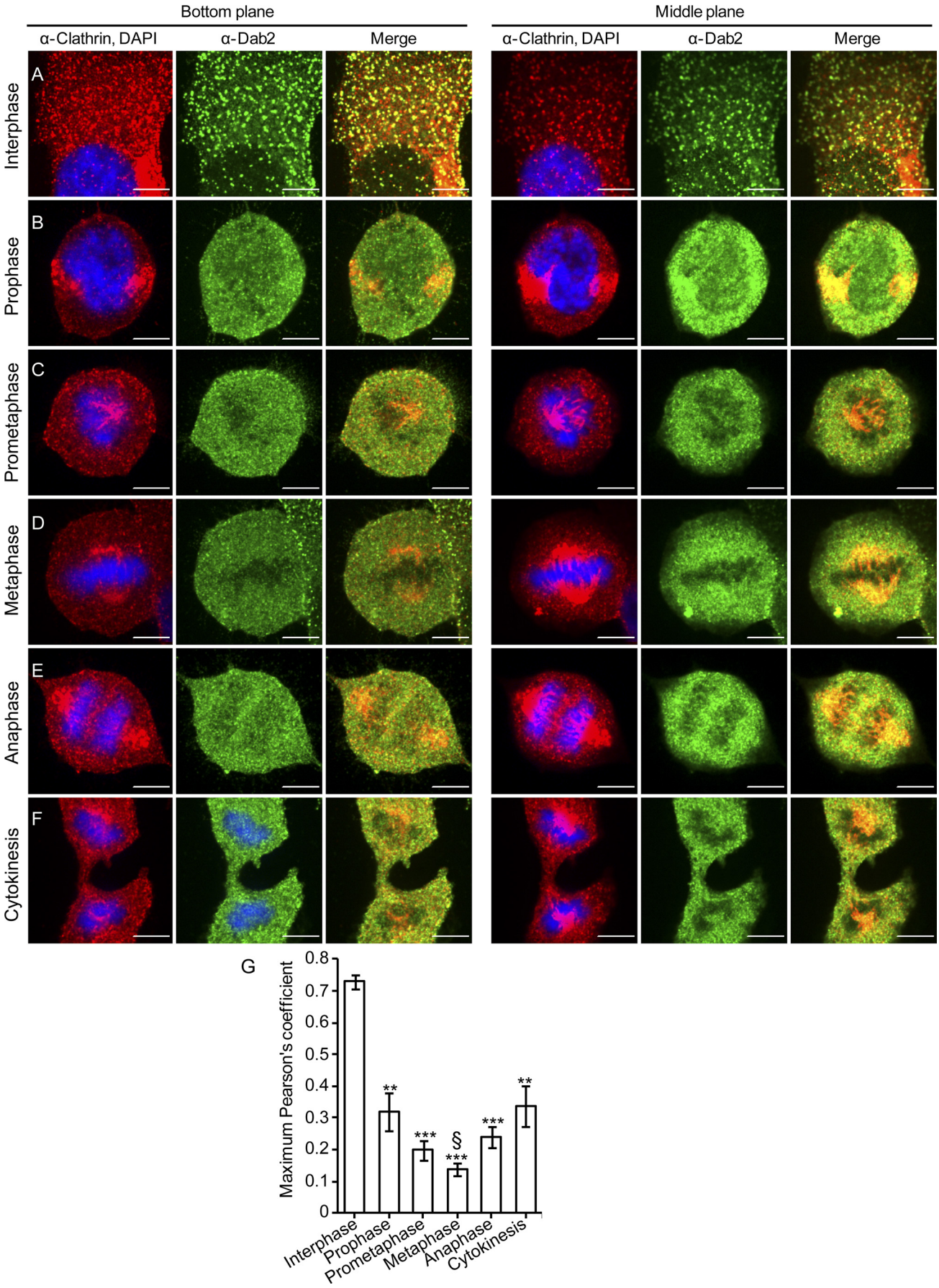
Bottom plane
Middle plane
α-Clathrin, DAPI
α-Dab2
Merge
α-Clathrin, DAPI
α-Dab2
Merge
A
Interphase
B
Prophase
C
Prometaphase
D
Metaphase
E
Anaphase
F
Cytokinesis
G
Maximum Pearson's coefficient
0.8
0.7
0.6
0.5
0.4
0.3
0.2
0.1
0
**
***
§
***
***
**
Interphase
Prophase
Prometaphase
Metaphase
Anaphase
Cytokinesis

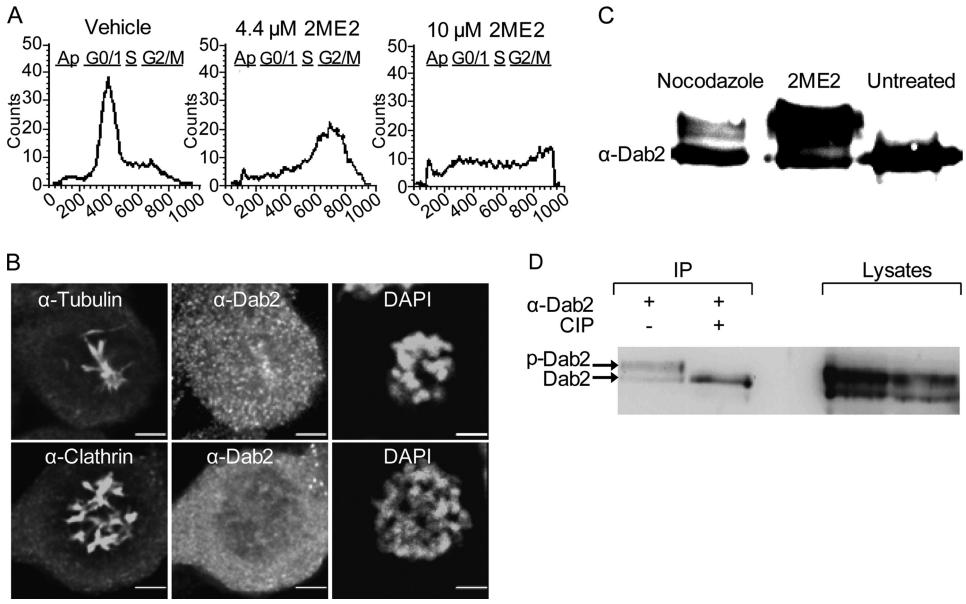

FIGURE 3. **2ME2 induces G_2/M arrest, the displacement of Dab2 from the membrane, and the phosphorylation of the p96 isoform of Dab2.** *A,* semi-confluent ES-2 cells were treated with 2ME2 (4.4 or 10 μM, 16 h) or the same amount of vehicle, suspended by scraping, and their DNA content was measured by propidium iodide staining and fluorescence-activated cell sorting (FACS). *B,* ES-2 cells, grown on glass coverslips, were treated with 2ME2 (4.4 μM, 16 h), fixed, permeabilized, and stained as indicated in the panels. *C,* semi-confluent ES-2 cells were treated with 2ME2 (4.4 μM, 16 h), nocodazole (50 μM, 16 h), or vehicle. Cells were lysed, resolved by SDS-PAGE, and immunoblotted with α-Dab2 antibodies *D,* semi-confluent ES-2 cells were treated for 16 h with 2ME2, lysed prior to immunoprecipitation with α-Dab2 antibodies. Precipitates were treated or not with calf intestinal phosphatase (*CIP*). Panel depicts a typical experiment ($n = 3$; the *two lanes* to the *left* are the immunoprecipitation (*IP*), and the *two lanes* to the *right* are 10% of the lysates employed).

(supplemental Fig. 3*C*). Thus, although the lack of a 2ME2-induced effect, when applied in combination with roscovitine, is in line with the results published by He *et al.* (43) and supports the notion that the 2ME2-induced effect occurs through the induction of mitotic arrest, our results fall short of attributing the phosphorylation of Dab2 exclusively to cdc2 kinase activity. The identification of additional kinase(s), which may modify Dab2, will be the object of future studies.

The central exon of the long isoform of Dab2 (spanning residues 230–447) contains its clathrin-binding motif (14). Recent studies, employing mass spectrometry, identify a cluster of residues (Ser-393, Ser-394, and Ser-401) that localize to this central exon and are phosphorylated in HeLa cells arrested in mitosis with nocodazole (52, 53). These data are in contrast to the proposed localization of the mitotic phosphorylation sites solely to the phosphotyrosine-binding domain (residues 1–233) and proline-rich domain (residues 600–730) domains of Dab2 (proposed by Ref. 43, based on an *in vitro* experiment employing cdc2). In addition, the residues Thr-221, Ser-227, and Ser-401 were identified as phosphoresidues in nuclearly localized Dab2 (54). Moreover, Ser-326 (55), Ser-324 and Thr-329 (53), and Ser-227, Thr-229, and Ser-231 were also identified as being cell cycle-regulated phosphorylation sites (53). Taken together, these data suggest the presence of clusters of phosphorylation sites in Dab2 (residues 221–231, 324–329, and 393–401) and raise the possibility that their phosphorylation is part of the mechanism by which its intracellular localization is regulated. To address the role of specific residues in the phosphorylation-dependent mobility shift of Dab2, we stably expressed Myc-tagged Dab2 constructs, which varied by the presence/absence of a subset of phosphorylatable residues, and assessed alterations to the shift in apparent molecular weight induced by 2ME2. Mutation of Ser-393, Ser-394, and Ser-401 to alanines (termed p82-3A) or deletion of the segment Ser-393 to Ser-401 (data not shown) significantly reduced the 2ME2-induced shift (a typical experiment is shown in Fig. 4*B*, $n = 5$). Additional serine/threonine to alanine mutations at residues 221 and 423 (termed p82-5A) did not add to the effect observed with the 3A construct (Fig. 4*B*), indicating that either these residues are not phosphorylated in mitosis or that their phosphorylation does not induce a shift in the apparent molecular weight of Dab2. The Rat-p82 isoform, employed as the basis for the generation of the Myc-Dab2 constructs (designated p82-WT-r), contains an asparagine at position 227, in contrast to the serine present in this position in mice and humans (Fig. 4*A*). To assess the possible role of this residue in the 2ME2-induced shift, we mutated the asparagine to serine (designated p82-WT-h). No significant differences in migration in SDS-PAGE were consistently observed among p82-WT-h and p82-WT-r (Fig. 4*B*). Taken together, these data point to the Ser-393–Ser-401 cluster as a regulatory site for 2ME2-induced

FIGURE 2. **Marked reduction in the co-localization of Dab2 and clathrin in mitotic cells.** Unsynchronized ES-2 cells were plated onto glass coverslips. 16 h post-plating, cells were fixed and stained against clathrin, Dab2, and DNA. Cells were imaged by confocal microscopy and assigned different stages of the cell cycle according to the DNA distribution pattern. *Bar,* 10 μm. *G, graph* depicts the quantification of the maximal Pearson's CCF of the fluorescence signals of Dab2 and clathrin in the bottom planes of cells imaged as in *A–F*. Values were calculated with ImageJ software. Each *bar* represents the average of 10–17 cells imaged in each condition. Significance was calculated by the Student's *t* test. ***, $p < 1E\text{-}6$; **, $p < 0.001$, both when comparing the average CCF values obtained in all cell cycle stages to the average CCF obtained in interphase cells; §, $p < 0.05$, when comparing the average CCF observed in metaphase cells to the average CCF value obtained in cells in cytokinesis or prophase.

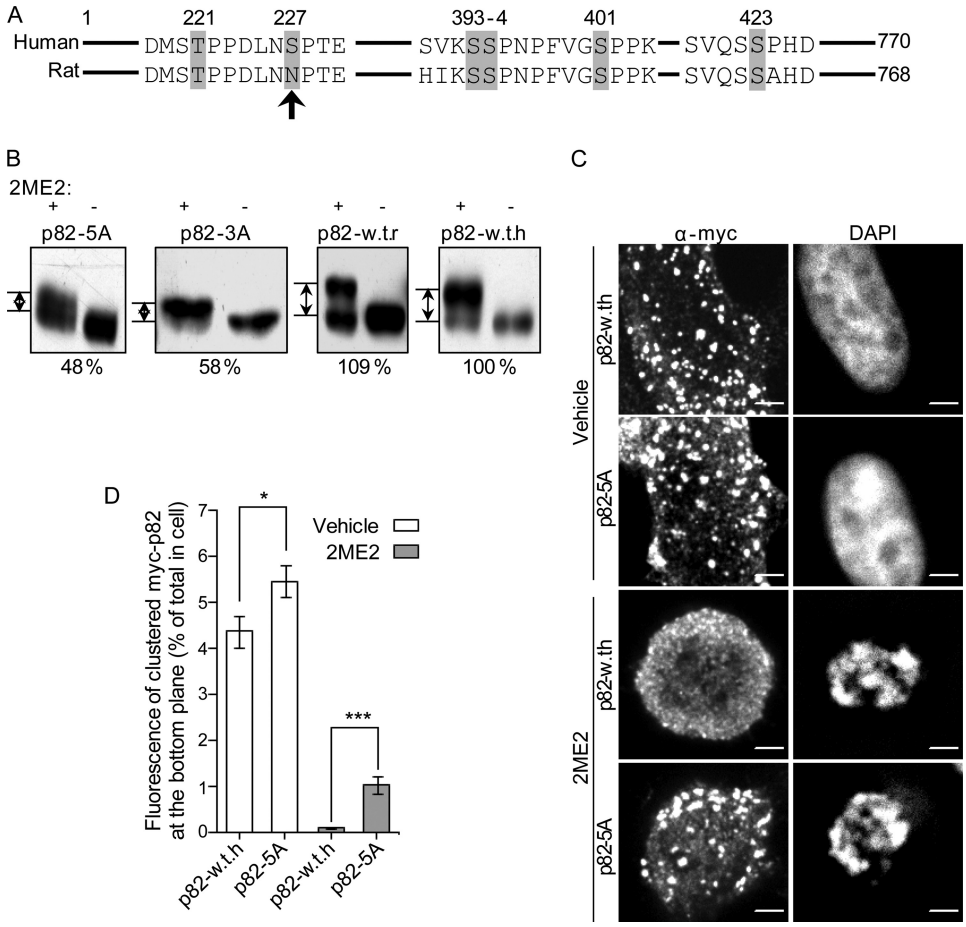

FIGURE 4. **Mutation of phosphorylatable sites in Dab2 reduces the 2ME2-induced shift in migration and displacement of Dab2 from the membrane.** *A,* schematic depiction of the central region of the human and rat p96/p82 isoforms of Dab2. Phosphorylatable sites that were mutated in this study are highlighted in *gray*. *Arrow* points to position 227, which differs among the human and rat isoforms and was mutated to serine on a rat Myc-p82 background (p82-WT-r) generating p82-WT-h. *B,* mutation of serines Ser-393, Ser-394, and Ser-401 to alanines reduces the 2ME2-induced shift in migration in SDS-PAGE. Single clones of ES-2 cells stably expressing the different Myc-p82-based constructs were treated or not with 2ME2 (4.4 μM, 16 h). Cell lysates (prepared as in Fig. 3) were separated by SDS-PAGE and immunoblotted with α-Myc antibodies. Panels depict a representative experiment ($n = 5$). All pairs of treated/untreated cells originate from the same gel and are presented separately due to different brightness/contrast adjustments. The measurement of the distance between the unphosphorylated and the phosphorylated bands of each construct (relative to p82-WT-h) appears *below* each panel. Similar values were obtained in all repeats of the experiment. *C,* p82-WT-h and p82-5A cells were plated onto glass coverslips and treated with 2ME2 (4.4 μM, 16 h) or vehicle. Cells were fixed, permeabilized, and stained with DAPI and α-Myc antibodies. Panels depict the bottom confocal plane of representative cells in each condition. *D,* quantification of the percentage of the Myc-p82 fluorescence signal present as clusters in the bottom plane of the cell. Results are average $\pm$ S.E. of three experiments. *White columns* represent vehicle-treated cells (45 cells per column), and *gray columns* represent 2ME2-treated cells (96 cells per column); *, $p < 0.05$; ***, $p < 0.00001$.

phosphorylation. However, the 2ME2-induced apparent molecular weight shift that is still observed with the both p82-3A and p82-5A is indicative of additional mitotic phosphorylation sites on Dab2. Accordingly, 2ME2 induced a considerable shift in the migration of a Myc-tagged construct of p67/p59 (supplemental Fig. 5*B*), suggesting that these additional site/sites may localize to regions other than the central exon of p96/p82. To directly probe for the identity of phosphorylated residues in p82-WT-h and p82-5A, we treated cells with 2ME2, immunoprecipitated the Myc-p82 constructs, separated them by SDS-PAGE, and processed them for mass spectrometry (see supplemental :Experimental Procedures"). Under the conditions employed here, only two phosphorylation sites were identified in p82-WT-h. In the 2ME2-treated sample, Ser-326 (and/or Ser-328) was phosphorylated (we cannot assign with certainty the identity of the phosphorylated residue). In contrast, in cycling cells, p82-WT-h was exclusively phosphorylated on Ser-401. Importantly, p82-5A (which is devoid of Ser-401 but endowed with both Ser-326 and Ser-328) showed no phosphorylation under either condition (supplemental Fig. 4). The identification and characterization by mass spectrometry of peptides that present multiple phosphorylations can be technically challenging (53).[3] Specifically, the localization of the candidate phosphorylated residues in Dab2 to clusters of adjacent residues (52–55) may lead to a potential difficulty in their identification by mass spectrometry (a possible reason for the variability among the different studies). As such, we employed a complementary approach that made use of the fact that a number of the candidate sites in Dab2 are adjacent to proline residues, enabling their identification with an antibody that specifically recognizes phosphorylated threonines and serines when adjacent to proline (a rabbit polyclonal antibody directed against phosphothreo-

[3] T. Ziv, personal communication.

nine-proline/phosphoserine-proline (Thr(P)-Pro/Ser(P)-Pro)). Lysates from cell lines stably expressing p82-WT-h, p82-5A, or p59-WT-r (a Myc-tagged construct of the Rat p59 isoform of Dab2), treated or not with 2ME2, were immunoprecipitated with a α-Myc antibody and sequentially immunoblotted with a α-Myc antibody and with the α-Thr(P)-Pro/Ser(P)-Pro antibody. In a typical experiment, in cells expressing p82-WT-h, 2ME2 induced an ~3-fold increase in the ratio of the α-Thr(P)-Pro/Ser(P)-Pro and the α-Myc signals (supplemental Fig. 5). Importantly, neither of the candidate sites identified by mass spectrometry (Ser-326 or Ser-328) is followed by a proline. Thus, this increase in signal ratio is indicative of the 2ME2-induced phosphorylation of additional residue(s), localized to the vicinity of prolines, and present in p82-WT-h.

Next, we examined, with a two-pronged approach, if the partial reduction in 2ME2-induced phosphorylation of p82-5A correlated with a lesser alteration to its intracellular localization. Initially, ES-2 cells, stably expressing p82-5A or p82-WT-h, were treated or not with 2ME2 and processed for immunofluorescence with anti-Myc antibodies. Stained cells were imaged by confocal microscopy, and the percentage of anti-Myc staining localized to membrane-bound punctate structures was calculated as in Ref. 49. 2ME2 induced a significant displacement from the membrane of both p82-WT-h and p82-5A. However, the extent of displacement of p82-5A is significantly reduced as compared with p82-WT-h (Fig. 4, *C* and *D*). In addition, we submitted ES-2 cells, expressing p82-WT-h or p82-5A and treated or not with 2ME2, to fractionation. Here too, 2ME2 increased the localization of the Myc-tagged constructs to the cytoplasmic fraction (with a lesser effect being observed with p82-5A) and markedly reduced the amount of p82-WT-h in the membrane fraction (supplemental Fig. 2*B*). Accordingly, immunofluorescence analysis of the intracellular distribution of p82-5A and p82-WT-h in cycling/mitotic cells revealed that, in this cellular setting, a considerable amount of p82-5A is retained at the membrane (supplemental Fig. 6). Interestingly, alanine to aspartate phosphomimetic mutations, of the residues mutated in p82-5A, were insufficient to emulate the 2ME2-induced effect (data not shown); indicating that either the phosphomimetic mutation fails to resemble certain aspects of the phosphorylated residue or that modifications to additional sites are necessary for the displacement of Dab2 from the plasma membrane. Taken as a whole, the results obtained with the p82-WT-h and p82-5A constructs support a role for mitotic phosphorylation, on multiple sites, in mediating the displacement of Dab2 from the membrane.

Abrogation of the Dab2/Clathrin Interaction in G_2/M-arrested Cells—To probe if clathrin and Dab2 interact in ES-2 cells and to examine if this interaction is sensitive to the phosphorylation induced by 2ME2, we immunoprecipitated Dab2 from vehicle- or 2ME2-treated cells and probed for the co-immunoprecipitation of the clathrin heavy chain. A clear association between these proteins was observed in vehicle-treated cells (Fig. 5*A*). 2ME2 reduced the association of Dab2 with clathrin (Fig. 5*A*). This reduction is in full accord with

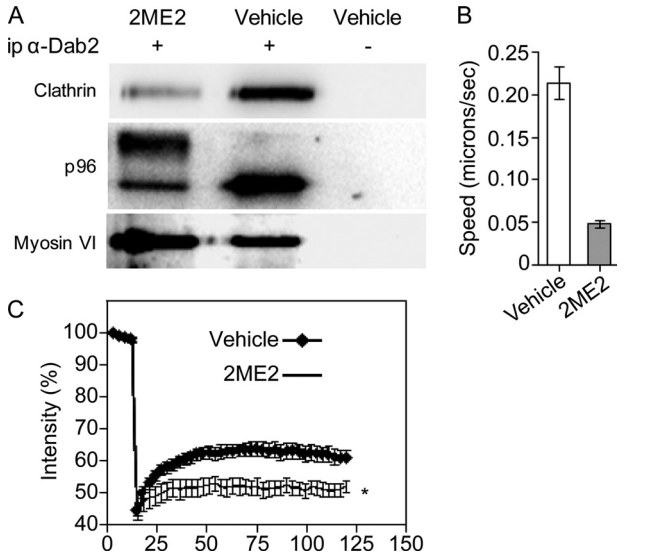

FIGURE 5. **2ME2 treatment reduces Dab2/clathrin interactions, decreases the movement of endocytic vesicles, and inhibits clathrin exchange.** *A,* lysates from ES-2 cells treated with 2ME2 (4.4 μM, 16 h) or vehicle were immunoprecipitated (*ip*) with rabbit-α-Dab2 antibody or a specificity control. Immunoprecipitates were resolved by SDS-PAGE and immunoblotted with mouse monoclonal α-Dab2, mouse-monoclonal α-clathrin, and rabbit- α-myosin VI. Panel depicts a representative experiment ($n = 4$). *B,* ES-2 cells were grown on glass coverslips and treated with 2ME2 (4.4 μM, 16 h) or vehicle. Cells were submitted to live uptake of transferrin (labeled with Alexa-555, 50 μg/ml, 37 °C). After 2 min of continuous uptake, cells were washed with imaging medium, and time lapse series (1 s between acquisitions) of confocal sections of regions adjacent to the cell membrane were acquired (up to 8 min after wash). *Bar graph* depicts the average ± S.E. of the mean square displacement of 250 vesicles, from 12 different cells per condition, from three independent experiments. *C,* ES-2 cells were grown on coverslips and transfected with clathrin light chain A fused to GFP (48). 24 h after transfection, cells were treated with 2ME2 (4.4 μM, 16 h) or vehicle. Cells were imaged by confocal microscopy and analyzed by fluorescence recovery after photobleaching (*FRAP*) (12 cells per condition, three independent experiments), both bleaching and analysis were carried out as in Ref. 49.

the lack of co-localization of Dab2 with clathrin in cells treated with 2ME2 (Fig. 3*B* and supplemental Fig. 3, *A* and *B*).

In addition to its interactions with clathrin, AP2, and receptors endowed with NP*X*Y signals, Dab2 mediates the recruitment of myosin VI to endocytic vesicles (25). To understand if the interaction between Dab2 and myosin VI is also abrogated by 2ME2, we probed for the co-immunoprecipitation of myosin VI and Dab2 in cells treated or not with 2ME2. Here, little to no effect was observed on the interaction of Dab2 and myosin VI (Fig. 5*A*). To test if 2ME2 entails modifications to endocytic vesicle motility, ES-2 cells (treated or not with 2ME2) were fed fluorescent transferrin (50 μM, 2 min). This was followed by up to 8 min "chase" (in medium devoid of transferrin), during which cells were continuously imaged (see supplemental movies 1 and 2). To enrich the population of early endocytic vesicles in the image analysis, only regions adjacent to the membrane (observed in the confocal sections) were employed for tracking and quantitation. Individual vesicles were tracked, and their mean square displacement was calculated. 2ME2 induced an ~75% reduction in vesicle displacement (Fig. 5*B*, $p < 1E\text{-}5$).

To test if the 2ME2-mediated mitotic arrest alters clathrin assembly dynamics, we employed fluorescence recovery after photobleaching and probed for the recovery parameters of

clathrin light chain A fused to GFP, transiently expressed in ES-2 cells treated or not with 2ME2 (4.4 μM, 16 h). Treatment with 2ME2 led to a significant reduction in the percentage of exchangeable clathrin (Fig. 5*C*, 66% reduction in the extent recovery, $p < 0.05$ at multiple recovery time points). These data suggest that the mitosis-induced alterations to the localization and post-translational modifications of endocytic adaptors such as Dab2 may lead to differences in the recruitment of clathrin to coated pits.

Selective Reduction of NPXY-based Endocytosis in Mitosis—Dab2 is a cargo-specific endocytic adaptor (13–15, 49). We hypothesized that the reduction in the amount of membrane-bound and coated pit-associated Dab2 should entail a reduction in the internalization of cargo endowed with an NP*X*Y endocytic signal. To test this hypothesis, we employed model receptors, based on a Myc-tagged truncation mutant of the TGF-β type I receptor, which is originally devoid of endocytic signals but can be supplemented with short sequences that lead to a gain-of-endocytic-function (49). To compare the endocytosis of the different receptors in interphase cells and in cells arrested in G_2/M, ES-2 cells were transfected with the different receptors; 24 h after transfection, cells were treated with either 2ME2 (4.4 μM, 16 h) or the same amount of vehicle. Cells were then fed Alexa-555-labeled monoclonal anti-Myc antibody (20 min, 37 °C, to allow endocytosis) after which cells were cooled to 4 °C, and the anti-Myc antibody attached to the cell surface was labeled with Alexa-488-labeled goat anti-mouse antibody. The entire volume of labeled cells was imaged by confocal microscopy, and the internal to total ratio of the red signal was calculated. Similarly to the recent report by Bocrout and Kirchhausen (35), an increase in the internalization of the receptor endowed with a Y*XX*Φ signal (also present in the transferrin receptor) was observed in cells arrested with 2ME2 (46 ± 5.3% increase, $p <$ 5E-5; Fig. 6*B*). In contrast, 2ME2 induced a marked reduction (75% ± 2.4%, $p <$ 5E-5) in the internalization of TβRI-LDLR (endowed with a FDNPXY signal). In these conditions, and in accord with its lack of internalization signals, no significant differences in the residual internalization of TβRI-158 were observed among vehicle and 2ME2-treated cells. Finally, to directly examine if the reduced displacement of p82-5A from the membrane in mitotic cells results in the retention of its endocytic function, we employed the ES-2-based cell lines expressing p82-WT-h and p82-5A and probed for the internalization of TβRI-158 and TβRI-LDLR. In cell lines expressing either Myc-p82 construct, 2ME2 induced a slight but significant reduction in the internalization of TβRI-158. The low levels of its internalization (in all conditions employed) allowed us to continue to view TβRI-158 as a negative control of the endocytosis mediated by the FDNP*X*Y motif. Importantly, in a sharp contrast to the reduction in TβRI-LDLR endocytosis observed in p82-WT-h-expressing cells treated with 2ME2 (84.3 ± 2.6% reduction, $p <$ p<9E-9), the stable expression of p82-5A leads to the abrogation of the 2ME2-induced effect and to the continued internalization of TβRI-LDLR in mitotic cells ($p > 0.89$).

DISCUSSION

The notion that the intracellular localization, repertoire of interactions, and function of Dab2 are altered in mitosis is supported by the following lines of evidence: (i) in interphase cells, the intracellular distribution of Dab2 yields a punctate staining characterized by a high variance to mean ratio (VtM); this staining pattern is lost throughout the mitosis of cycling cells and in cells arrested at the SAC with 2ME2, where a diffuse staining pattern is characterized by a low VtM. Importantly, the VtM obtained under these latter conditions is similar to the one observed in the interior of the cell, further supporting the notion of the displacement of Dab2 to the cytosol in mitosis (Fig. 1 and supplemental Fig. 1). Moreover, the distribution pattern of Dab2 in cells in cytokinesis yields an intermediate VtM value (Fig. 1 and supplemental Fig. 1), stressing the cyclical nature of the displacement of Dab2 in the cell cycle. The notion of the displacement of Dab2 to the cytosol is further supported by the 2ME2-induced alterations observed by cell fractionation (supplemental Fig. 2). (ii) At the plasma membrane of interphase cells, Dab2 and clathrin show a high degree of co-localization, reflected by the high value of the maximal Pearson's CCF of their fluorescence signals. In the course of mitosis, this CCF is significantly reduced (Fig. 2*G*). Here too, 2ME2-mediated cell cycle arrest emulated the effects observed in mitotic/cycling cells (supplemental Fig. 3*B*), reinforcing the notion of its appropriateness as a means of enrichment of the mitotic cell population. Importantly, in mitosis, clathrin and Dab2 accumulated in different intracellular compartments. Although clathrin showed a prominent recruitment to the mitotic spindle, Dab2 remained diffuse in the cytoplasm of the cell (Figs. 2 and 3*B*). Here too, the CCF value obtained in cytokinesis is significantly higher than the minimal value, observed in cells in metaphase (Fig. 2*G*), reinforcing the notion of the cyclical regulation of Dab2/clathrin interactions. (iii) Dab2 and clathrin co-immunoprecipitate in interphase cells, an interaction that is lost in 2ME2-treated cells (Fig. 5). In contrast, the interaction between Dab2 and myosin VI is maintained in the mitotically arrested cells (Fig. 5*A*), stressing the specificity of the abrogation of Dab2-clathrin interactions in mitosis. The interaction of Dab2 with myosin VI is mediated through the C-terminal region of Dab2 (56, 57), whereas the sequence involved in binding to clathrin localizes to the central exon of Dab2 (14). Importantly, in mitosis, myosin VI also undergoes marked changes to its intracellular localization and performs important roles, related to membrane traffic in cytokinesis (58). (iv) In 2ME2-arrested cells, Dab2 is extensively phosphorylated. This phosphorylation induced a marked shift in the migration of Dab2 in SDS-PAGE, a shift that is abolished by incubation with calf intestinal phosphatase (Fig. 3*D*). Moreover, the mutation of Ser-393, Ser-394, and Ser-401 to alanines or the deletion of these residues reduced this shift in migration (Fig. 4*B*). A comparative mass spectrometry analysis of the phosphorylation of p82-WT-h in vehicle/2ME2-treated cells revealed the 2ME2-induced phosphorylation of Ser-326 (or Ser-328). Importantly, these sites, which are present in p82-5A, were not phosphorylated in this molecular context in 2ME2-arrested cells

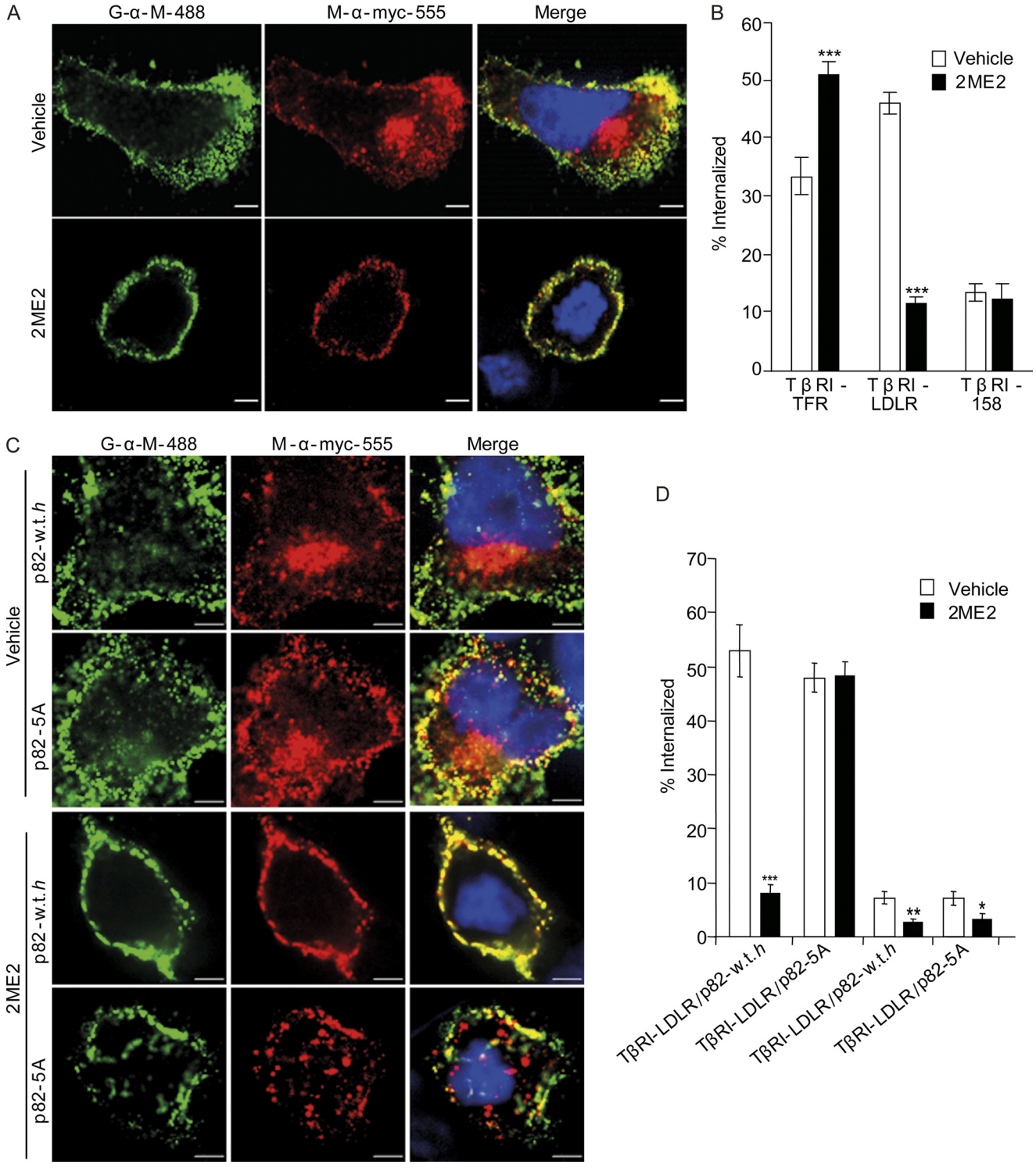

FIGURE 6. **2ME2-mediated cell cycle arrest leads to a specific decrease in the internalization of a receptor with an NPXY endocytic signal.** *A,* ES-2 cells were transfected with the different constructs, based on an epitope-tagged endocytosis-negative truncation mutant of the type I TGF-β receptor (TβRI-158), supplemented or not with either a *YXXΦ* (TβRI-transferring receptor) or an NP*X*Y-based signal (TβRI-LDLR; all constructs are described in Ref. 49). 24–30 h after transfection, cells were treated with either 2ME2 (4.4 μM, 16 h) or vehicle. Subsequently, cells were fed Alexa-555-labeled α-Myc (9E10) antibodies (20 μg/ml, 20 min, 37 °C) before being cooled and labeled with Alexa-488 goat-α-mouse (20 μg/ml, 60 min, 4 °C). The entire cell volume of cells was acquired by confocal microscopy. Intensity-based segmentation was employed for signal identification, and co-localized signal-positive pixels were determined with Slidebook™. *Bar,* 5 μm. *B, graph* depicts the average ± S.E. of internal to total ratio of the Alexa-555 signal, from three independent experiments (a total of ~60 cells per condition). *C,* ES-2 cells, doubly transfected with TβRI-LDLR or TβRI-158 and p82-WT-h or p82-5A, were treated and processed as in *A*. Panels depict typical cells in each condition. *Bar,* 5 μm. *D, graph* depicts the average ± S.E. of internal to total ratio of the Alexa-555 signal, from two independent experiments (a total of 30–40 cells per condition; ***, $p < 9E-9$; **, $p < 4E-3$; *, $p < 5E-2$).

(supplemental Fig. 4). Moreover, p82-WT-h also shows significant phosphorylation on Thr(P)-Pro/Ser(P)-Pro sites (supplemental Fig. 5), suggesting that Ser-326 (or Ser-328), which is not adjacent to prolines, are not the sole sites of its mitotic phosphorylation. Furthermore, the reduction in the phosphorylation of p82-5A correlated with the decrease in its displacement from the membrane (supplemental Fig. 2) and with its continued localization to membrane-bound punctate structures in 2ME2-treated cells (Fig. 4, *C* and *D*) and in cycling cells in mitosis (supplemental Fig. 6). (v) In 2ME2-treated cells, the internalization of a receptor endowed with an FDNP*X*Y endocytic motif is specifically inhibited (Fig. 6). Importantly, the 2ME2-induced reduction in the internalization of this receptor is dependent on the displacement of Dab2 from the membrane, as it is rescued in p82-5A-expressing cells (Fig. 6, *C* and *D*). Accordingly, we have previously shown that the internalization of this same construct is enhanced upon the expression of GFP-Dab2 in COS7 cells (49). Importantly, and similarly to what was reported by Boucrot and Kirchhausen (35), the internalization of an analogous TβRI-based construct endowed with a Y*XX*Φ-like endocytic signal, which is supposedly entirely dependent on AP2, was not reduced in cells arrested in mitosis with 2ME2 (Fig. 6). Thus, arrest of cells in mitosis affects the internalization of only a subpopulation of receptors.

In addition to Dab2, epsin and Eps15 are also phosphorylated in G_2/M (42, 59, 60). Interestingly, the phosphorylation of both epsin and Eps15 also leads to a decrease in their endocytic function, through the reduction in their interaction with AP2/clathrin (42). This negative regulation of endocytic proteins in mitosis contrasts with the functionality of AP2/clathrin throughout mitosis (35) and suggests a differential regulation of endocytic "auxiliary factors" as compared with those defined as "endocytic hubs" (according to the clathrin interactome in Ref. 61). What are putative causes and consequences of this selectivity? (i) The mitotic cell alters the extent and possibly the nature of its interactions with its neighboring cells, with the extracellular matrix, and with its microenvironment. This dynamic process may demand an alteration in the repertoire of receptors exposed at the cell surface. Selective inhibition of the internalization of a subset of receptors, in the context of a general reduction in surface area (35, 62), may be a way of achieving this modulation. (ii) Endocytic proteins perform alternative functions in mitotic cells. Prominent examples of this phenomenon are the recruitment of clathrin to the mitotic spindle (38, 39), the association of the endocytic adaptor ARH with centrosomal proteins (63), and the nonendocytic functions performed by epsin in mitosis (64). (iii) The mitotic cell is a different physicochemical environment than the interphase cell and may thus present different requirements for the regulation of coated pit/coated vesicle formation. For example, mitotic cells have a reduced volume (62, 65), enhanced membrane tension (36), and a different organization of the actin cytoskeleton (66), all of which potentially alter endocytosis. Specifically, we employed spinning disk confocal microscopy to measure the volume of ES-2 cells in metaphase and in 2ME2-mediated mitotic arrest, and we found that their volume is reduced by ~60% in these conditions (data not shown). Such a reduction in volume would imply that the concentration of long lived proteins (the reported half-lives of clathrin and Dab2 are ~50 and ~16 h, respectively (10, 67)) may be 3-fold higher under these conditions. Interestingly, the endocytic machinery is sensitive to alterations in clathrin concentration (68). Moreover, although basic cell functions are not affected in the absence of Dab2, which is down-regulated/depleted in the initial phases of tumorigenesis of many tumor types (1, 69), an increase in the amounts of Dab2 leads to profound alterations to the organization of clathrin in cells (49, 70). Also, overexpression of epsin1 leads to a decrease in clathrin-mediated endocytosis (71). Interestingly, incubation of cells in hypertonic medium (0.45 M sucrose), which reduces cell volume (by ~50%, data not shown), induces a massive polymerization of clathrin and Dab2 into unproductive structures (49, 72). Thus, a reduction in interactions with the membrane and with clathrin, through mitotic phosphorylation, may be a manner of reducing the concentration of active Dab2 and possibly also of additional auxiliary endocytic factors such as epsin and Eps15. This reduction may be part of a regulatory mechanism aimed at the continuation of endocytosis (of a subset of receptors) in mitosis, despite the broad alterations to the physicochemical environment of the cell.

Acknowledgment—Mass spectrometry was performed at the Smoler Proteomics Center at the Technion-Israel Institute of Technology, Haifa, Israel.

REFERENCES

1. Wang, Z., Tseng, C. P., Pong, R. C., Chen, H., McConnell, J. D., Navone, N., and Hsieh, J. T. (2002) *J. Biol. Chem.* **277,** 12622–12631
2. Cho, S. Y., Jeon, J. W., Lee, S. H., and Park, S. S. (2000) *Biochem. J.* **352,** 645–650
3. Huang, C. H., Cheng, J. C., Chen, J. C., and Tseng, C. P. (2007) *Cell. Signal.* **19,** 1339–1347
4. Xu, X. X., Yi, T., Tang, B., and Lambeth, J. D. (1998) *Oncogene* **16,** 1561–1569
5. Zhou, J., and Hsieh, J. T. (2001) *J. Biol. Chem.* **276,** 27793–27798
6. Zhou, J., Scholes, J., and Hsieh, J. T. (2003) *J. Biol. Chem.* **278,** 6936–6941
7. Jiang, Y., Prunier, C., and Howe, P. H. (2008) *Oncogene* **27,** 1865–1875
8. Hocevar, B. A., Mou, F., Rennolds, J. L., Morris, S. M., Cooper, J. A., and Howe, P. H. (2003) *EMBO J.* **22,** 3084–3094
9. Hocevar, B. A., Prunier, C., and Howe, P. H. (2005) *J. Biol. Chem.* **280,** 25920–25927
10. Hocevar, B. A., Smine, A., Xu, X. X., and Howe, P. H. (2001) *EMBO J.* **20,** 2789–2801
11. Prunier, C., and Howe, P. H. (2005) *J. Biol. Chem.* **280,** 17540–17548
12. Yang, D. H., Smith, E. R., Roland, I. H., Sheng, Z., He, J., Martin, W. D., Hamilton, T. C., Lambeth, J. D., and Xu, X. X. (2002) *Dev. Biol.* **251,** 27–44
13. Keyel, P. A., Mishra, S. K., Roth, R., Heuser, J. E., Watkins, S. C., and Traub, L. M. (2006) *Mol. Biol. Cell* **17,** 4300–4317
14. Mishra, S. K., Keyel, P. A., Hawryluk, M. J., Agostinelli, N. R., Watkins, S. C., and Traub, L. M. (2002) *EMBO J.* **21,** 4915–4926
15. Maurer, M. E., and Cooper, J. A. (2006) *J. Cell Sci.* **119,** 4235–4246
16. Maurer, M. E., and Cooper, J. A. (2005) *J. Cell Sci.* **118,** 5345–5355
17. Nagai, J., Christensen, E. I., Morris, S. M., Willnow, T. E., Cooper, J. A., and Nielsen, R. (2005) *Am. J. Physiol. Renal Physiol.* **289,** F569–F576
18. Morris, S. M., Arden, S. D., Roberts, R. C., Kendrick-Jones, J., Cooper, J. A., Luzio, J. P., and Buss, F. (2002) *Traffic* **3,** 331–341

19. Morris, S. M., Tallquist, M. D., Rock, C. O., and Cooper, J. A. (2002) *EMBO J.* **21,** 1555–1564
20. Morris, S. M., and Cooper, J. A. (2001) *Traffic* **2,** 111–123
21. Cuitino, L., Matute, R., Retamal, C., Bu, G., Inestrosa, N. C., and Marzolo, M. P. (2005) *Traffic* **6,** 820–838
22. Xu, X. X., Yang, W., Jackowski, S., and Rock, C. O. (1995) *J. Biol. Chem* **270,** 14184–14191
23. Hasson, T. (2003) *J. Cell Sci.* **116,** 3453–3461
24. Dance, A. L., Miller, M., Seragaki, S., Aryal, P., White, B., Aschenbrenner, L., and Hasson, T. (2004) *Traffic* **5,** 798–813
25. Spudich, G., Chibalina, M. V., Au, J. S., Arden, S. D., Buss, F., and Kendrick-Jones, J. (2007) *Nat. Cell Biol.* **9,** 176–183
26. Kowanetz, K., Terzic, J., and Dikic, I. (2003) *FEBS Lett.* **554,** 81–87
27. Chao, W. T., and Kunz, J. (2009) *FEBS Lett.* **583,** 1337–1343
28. Huang, C. L., Cheng, J. C., Stern, A., Hsieh, J. T., Liao, C. H., and Tseng, C. P. (2006) *J. Cell Sci.* **119,** 4420–4430
29. Calderwood, D. A., Fujioka, Y., de Pereda, J. M., García-Alvarez, B., Nakamoto, T., Margolis, B., McGlade, C. J., Liddington, R. C., and Ginsberg, M. H. (2003) *Proc. Natl. Acad. Sci. U.S.A.* **100,** 2272–2277
30. Teckchandani, A., Toida, N., Goodchild, J., Henderson, C., Watts, J., Wollscheid, B., and Cooper, J. A. (2009) *J. Cell Biol.* **186,** 99–111
31. Warren, G., Davoust, J., and Cockcroft, A. (1984) *EMBO J.* **3,** 2217–2225
32. Pypaert, M., Lucocq, J. M., and Warren, G. (1987) *Eur. J. Cell Biol.* **45,** 23–29
33. Pypaert, M., Mundy, D., Souter, E., Labbé, J. C., and Warren, G. (1991) *J. Cell Biol.* **114,** 1159–1166
34. Schweitzer, J. K., Burke, E. E., Goodson, H. V., and D'Souza-Schorey, C. (2005) *J. Biol. Chem.* **280,** 41628–41635
35. Boucrot, E., and Kirchhausen, T. (2007) *Proc. Natl. Acad. Sci. U.S.A.* **104,** 7939–7944
36. Raucher, D., and Sheetz, M. P. (1999) *J. Cell Biol.* **144,** 497–506
37. Borlido, J., Veltri, G., Jackson, A. P., and Mills, I. G. (2008) *PLoS ONE* **3,** e3115
38. Yamauchi, T., Ishidao, T., Nomura, T., Shinagawa, T., Tanaka, Y., Yonemura, S., and Ishii, S. (2008) *EMBO J.* **27,** 1852–1862
39. Royle, S. J., Bright, N. A., and Lagnado, L. (2005) *Nature* **434,** 1152–1157
40. Okamoto, C. T., McKinney, J., and Jeng, Y. Y. (2000) *Am. J. Physiol. Cell Physiol.* **279,** C369–C374
41. Albertson, R., Riggs, B., and Sullivan, W. (2005) *Trends Cell Biol.* **15,** 92–101
42. Chen, H., Slepnev, V. I., Di Fiore, P. P., and De Camilli, P. (1999) *J. Biol. Chem.* **274,** 3257–3260
43. He, J., Xu, J., Xu, X. X., and Hall, R. A. (2003) *Oncogene* **22,** 4524–4530
44. Musacchio, A., and Salmon, E. D. (2007) *Nat. Rev. Mol. Cell Biol.* **8,** 379–393
45. Jordan, M. A., Thrower, D., and Wilson, L. (1992) *J. Cell Sci.* **102**, 401–416
46. Attalla, H., Mäkelä, T. P., Adlercreutz, H., and Andersson, L. C. (1996) *Biochem. Biophys. Res. Commun.* **228,** 467–473
47. Kamath, K., Okouneva, T., Larson, G., Panda, D., Wilson, L., and Jordan, M. A. (2006) *Mol. Cancer Ther.* **5,** 2225–2233
48. Ehrlich, M., Boll, W., Van Oijen, A., Hariharan, R., Chandran, K., Nibert, M. L., and Kirchhausen, T. (2004) *Cell* **118,** 591–605
49. Chetrit, D., Ziv, N., and Ehrlich, M. (2009) *Biochem. J.* **418,** 701–715
50. Keydar, I., Chou, C. S., Hareuveni, M., Tsarfaty, I., Sahar, E., Selzer, G., Chaitchik, S., and Hizi, A. (1989) *Proc. Natl. Acad. Sci. U.S.A.* **86,** 1362–1366
51. Pribluda, V. S., Gubish, E. R., Jr., Lavallee, T. M., Treston, A., Swartz, G. M., and Green, S. J. (2000) *Cancer Metastasis Rev.* **19,** 173–179
52. Beausoleil, S. A., Villén, J., Gerber, S. A., Rush, J., and Gygi, S. P. (2006) *Nat. Biotechnol.* **24,** 1285–1292
53. Olsen, J. V., Vermeulen, M., Santamaria, A., Kumar, C., Miller, M. L., Jensen, L. J., Gnad, F., Cox, J., Jensen, T. S., Nigg, E. A., Brunak, S., and Mann, M. (2010) *Sci. Signal.* **3,** ra3
54. Beausoleil, S. A., Jedrychowski, M., Schwartz, D., Elias, J. E., Villén, J., Li, J., Cohn, M. A., Cantley, L. C., and Gygi, S. P. (2004) *Proc. Natl. Acad. Sci. U.S.A.* **101,** 12130–12135
55. Dephoure, N., Zhou, C., Villén, J., Beausoleil, S. A., Bakalarski, C. E., Elledge, S. J., and Gygi, S. P. (2008) *Proc. Natl. Acad. Sci. U.S.A.* **105,** 10762–10767
56. Phichith, D., Travaglia, M., Yang, Z., Liu, X., Zong, A. B., Safer, D., and Sweeney, H. L. (2009) *Proc. Natl. Acad. Sci. U.S.A.* **106,** 17320–17324
57. Yu, C., Feng, W., Wei, Z., Miyanoiri, Y., Wen, W., Zhao, Y., and Zhang, M. (2009) *Cell* **138,** 537–548
58. Arden, S. D., Puri, C., Au, J. S., Kendrick-Jones, J., and Buss, F. (2007) *Mol. Biol. Cell* **18,** 4750–4761
59. Rossé, C., L'Hoste, S., Offner, N., Picard, A., and Camonis, J. (2003) *J. Biol. Chem.* **278,** 30597–30604
60. Kariya, K., Koyama, S., Nakashima, S., Oshiro, T., Morinaka, K., and Kikuchi, A. (2000) *J. Biol. Chem.* **275,** 18399–18406
61. Schmid, E. M., and McMahon, H. T. (2007) *Nature* **448,** 883–888
62. Boucrot, E., and Kirchhausen, T. (2008) *PLoS ONE* **3,** e1477
63. Lehtonen, S., Shah, M., Nielsen, R., Iino, N., Ryan, J. J., Zhou, H., and Farquhar, M. G. (2008) *Mol. Biol. Cell* **19,** 2949–2961
64. Liu, Z., and Zheng, Y. (2009) *J. Cell Biol.* **186,** 473–480
65. Habela, C. W., and Sontheimer, H. (2007) *Cell Cycle* **6,** 1613–1620
66. Kunda, P., and Baum, B. (2009) *Trends Cell Biol.* **19,** 174–179
67. Acton, S. L., and Brodsky, F. M. (1990) *J. Cell Biol.* **111,** 1419–1426
68. Moskowitz, H. S., Yokoyama, C. T., and Ryan, T. A. (2005) *Mol Biol. Cell* **16,** 1769–1776
69. Karam, J. A., Shariat, S. F., Huang, H. Y., Pong, R. C., Ashfaq, R., Shapiro, E., Lotan, Y., Sagalowsky, A. I., Wu, X. R., and Hsieh, J. T. (2007) *Clin. Cancer Res.* **13,** 4400–4406
70. Mettlen, M., Loerke, D., Yarar, D., Danuser, G., and Schmid, S. L. (2010) *J. Cell Biol.* **188,** 919–933
71. Henne, W. M., Boucrot, E., Meinecke, M., Evergren, E., Vallis, Y., Mittal, R., and McMahon, H. T. (2010) *Science* **328,** 1281–1284
72. Heuser, J. E., and Anderson, R. G. (1989) *J. Cell Biol.* **108,** 389–400
73. Bolte, S., and Cordelières, F. P. (2006) *J. Microsc.* **224,** 213–232